

# Good Teachers Explain: Explanation-Enhanced Knowledge Distillation

Amin Parchami-Araghi\*, Moritz Böhle\*, Sukrut Rao\*, Bernt Schiele

Max Planck Institute for Informatics, Saarland Informatics Campus, Saarbrücken, Germany

{mparcham,mboehle,sukrut.rao,schiele}@mpi-inf.mpg.de

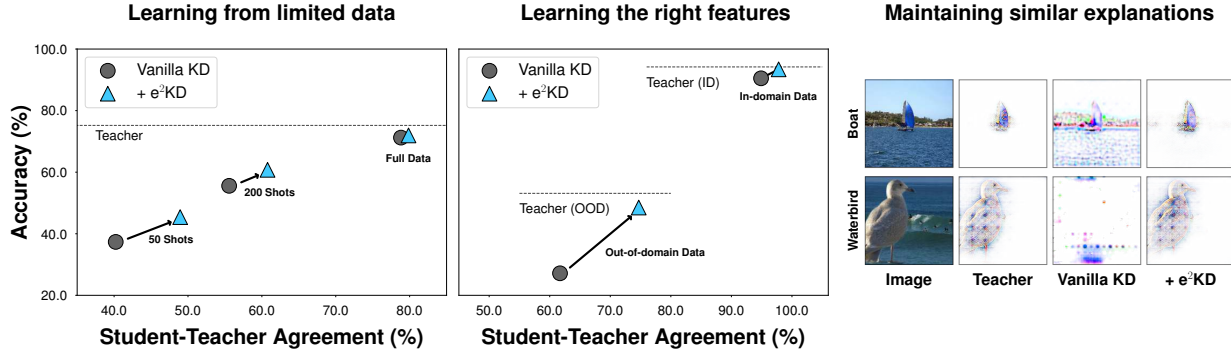


Figure 1. **A good teacher explains.** Using explanation-enhanced KD (e<sup>2</sup>KD) can improve KD fidelity and student performance. E.g., e<sup>2</sup>KD allows the student models to more faithfully approximate the teacher, especially when using fewer data, leading to large gains in accuracy and agreement between teacher and student (**left**). Further, by guiding the students to give the same explanations as the teachers, e<sup>2</sup>KD ensures that students learn to be ‘right for the right reasons’, improving their accuracy under distribution shifts (**center**). Lastly, e<sup>2</sup>KD students learn similar explanations as the teachers, thus exhibiting a similar degree of interpretability as the teacher (**right**).

## Abstract

Knowledge Distillation (KD) has proven effective for compressing large teacher models into smaller student models. While it is well known that student models can achieve similar accuracies as the teachers, it has also been shown that they nonetheless often do not learn the same function [40]. It is, however, often highly desirable that the student’s and teacher’s functions share similar properties such as basing the prediction on the same input features, as this ensures that students learn the ‘right features’ from the teachers. In this work, we explore whether this can be achieved by not only optimizing the classic KD loss but also the similarity of the explanations generated by the teacher and the student. Despite the idea being simple and intuitive, we find that our proposed ‘explanation-enhanced’ KD (e<sup>2</sup>KD) (1) consistently provides large gains in terms of accuracy and student-teacher agreement, (2) ensures that the student learns from the teacher to be right for the right reasons and to give similar explanations, and (3) is robust with respect to the model architectures, the amount of training data, and even works with ‘approximate’, pre-computed explanations.<sup>1</sup>

\*Equal contribution.

<sup>1</sup>Code available at [github.com/m-parchami/GoodTeachersExplain](https://github.com/m-parchami/GoodTeachersExplain)

## 1. Introduction

Knowledge Distillation (KD) [21] has proven to be an effective scheme for improving classification accuracies of relatively small ‘student’ models, by training them to match the logit distribution of larger, more powerful ‘teacher’ models. Despite its simplicity, this approach can be sufficient for the students to match the teacher’s accuracy, while requiring only a fraction of the computational resources of the teacher [4]. Recent findings, however, show that while the students might match the teacher’s accuracy, the knowledge is nonetheless not distilled faithfully [40].

Faithful KD, i.e. a distillation that ensures that the teacher’s and the student’s functions share properties beyond classification accuracy, is however desirable for many reasons. E.g., the lack of agreement between models [40] can hurt the user experience when updating machine-learning-based applications [3, 42]. Similarly, if the students use different input features than the teachers, they might not be *right for the right reasons* [35]. Further, given the recent AI Act proposal by European legislators [10], it is likely that the interpretability of models will play an increasingly important role and become an intrinsic part of the model functionality. To maintain the *full* functionality of a model, KD should thus ensure that the students allow for

the same degree of model interpretability as the teachers.

To address this, in this work we study if promoting explanation similarity using commonly used model explanations such as GradCAM [37] or those of the recently proposed B-cos models [5] can increase KD fidelity. This should be the case if such explanations indeed reflect meaningful aspects of the models’ ‘internal reasoning’. Concretely, we propose ‘**explanation-enhanced**’ KD ( $e^2$ KD), a simple, parameter-free, and model-agnostic addition to KD in which we train the student to also match the teacher’s explanations.

Interestingly, despite its simplicity, we find  $e^2$ KD to significantly improve distillation fidelity in a variety of settings (Fig. 1). Specifically,  $e^2$ KD improves student accuracy by ensuring that the students learn to be right for the right reasons and inherently promotes consistent explanations between teachers and students. Moreover, the benefits of  $e^2$ KD are robust to limited data, approximate explanations, and across model architectures.

In summary, we make the following contributions:

- (1) We propose **explanation-enhanced KD** ( $e^2$ KD) and train the students to not only match the teachers’ logits, but also their explanations (Sec. 3.1). This not only yields highly competitive students in terms of accuracy, but also significantly improves KD fidelity on the ImageNet [12], Waterbirds-100 [30, 36], and PASCAL VOC [13] datasets.
- (2) We discuss three desiderata for measuring KD fidelity. In particular, we (a) evaluate whether the student is performant and has high agreement with the teacher (Sec. 3.2.1), (b) examine whether students learn to use the same input features as a teacher that was guided to be ‘right for the right reasons’ even when distilling with biased data (Sec. 3.2.2), and (c) explore whether they learn the same explanations and architectural priors as the teacher (Sec. 3.2.3).
- (3) We show  $e^2$ KD to be a robust approach for improving knowledge distillation, which provides consistent gains across model architectures and with limited data. Moreover,  $e^2$ KD is even robust to using cheaper ‘approximate’ explanations. Specifically, for this we propose using ‘**frozen explanations**’ which are only computed once and, during training, we apply any augmentations simultaneously to the image and the explanations (Sec. 3.3).

## 2. Related Work

**Knowledge Distillation (KD)** has been introduced to compress larger models into smaller, more efficient models for cost-effective deployment [21]. Various approaches for KD have since been proposed, which we group into three types for the following discussion: *logit*- [4, 21, 47], *feature*- [9, 34, 39, 45], and *explanation-based KD* [1, 19].

*Logit-based KD* [21], which optimizes the logit distributions of teacher and student to be similar, can suffice to match their accuracies, as long as the models are trained for long enough (‘patient teaching’) and the models’ logits are

based on the same images (‘consistent teaching’), see [4]. However, [40] showed that despite such a careful setup, the function learnt by the student can still significantly differ from the teacher’s by comparing the agreement between the two. We expand on [40] and introduce additional evaluation settings to better evaluate KD fidelity, and show that it can be significantly improved by a surprisingly simple explanation-matching approach. While [28] reports that KD does seem to transfer additional properties to the student, by showing that GradCAM explanations of the students are more similar to the teacher’s than those of an independently trained model, we show that explicitly optimizing for explanation similarity not only significantly improves this w.r.t. vanilla KD, but also yields important additional benefits such as a higher robustness to distribution shifts.

*Feature-based KD* approaches [9, 34, 39, 45] provide additional information to the students by optimizing some of the students’ intermediate activation maps to be similar to those of the teacher. For this, specific choices regarding which layers of teachers and students to match need to be made and these approaches are thus architecture-dependent. In contrast, our proposed  $e^2$ KD is architecture-agnostic as it matches only the explanations of the models’ predictions.

*Explanation-based KD* approaches have only recently begun to emerge [1, 19] and these are conceptually most related to our work. In CAT-KD [19], the authors match class activation maps (CAM [48]) of students and teachers. As such, CAT-KD can also be considered an ‘explanation-enhanced’ KD ( $e^2$ KD) approach. However, the explanation aspect of the CAMs plays only a secondary role in [19], as the authors even reduce the resolution of the CAMs to  $2 \times 2$  and fidelity is not considered. In contrast, we explicitly introduce  $e^2$ KD to improve distillation fidelity and evaluate fidelity across multiple settings. Further, similar to our work, [1] argues that explanations can form part of the model functionality and should be considered in KD. To do so, the authors train an additional autoencoder to mimic the explanations of the teacher model; explanations and predictions are thus produced by separate models. In contrast, we optimize the students directly to yield similar explanations as the teachers in a simple and parameter-free manner.

**Fixed Teaching.** [15, 38, 44] explore pre-computing the logits at the start of training to limit the computational costs due to the teacher. In addition to pre-computing *logits*, we pre-compute *explanations* and show how they can nonetheless be used to guide the student model during distillation.

**Explanation Methods.** To better understand the decision making process of DNNs, many explanation methods have been proposed in recent years [2, 5, 33, 37]. For our  $e^2$ KD experiments, we take advantage of the differentiability of attribution-based explanations and train the student models to yield similar explanations as the teachers. In particular, we evaluate both a popular post-hoc explanation method

(GradCAM [37]) as well as the model-inherent explanations of the recently proposed B-cos models [5, 6].

**Model Guidance.**  $e^2$ KD is inspired by recent advances in model guidance [17, 18, 30, 32, 35], where models are guided to focus on desired input features via human annotations. Analogously, we also guide the focus of student models, but using knowledge (explanations) of a teacher model instead of a human annotator. As such, no explicit guidance annotations are required in our approach. Further, in contrast to the discrete annotations typically used in model guidance (e.g. bounding boxes or segmentation masks), we use the real-valued explanations as given by the teacher model. Our approach thus shares additional similarities with [30], in which a model is guided via the attention maps of a vision-language model. Similar to our work, the authors show that this can guide the students to focus on the ‘right’ input features. We extend such guidance to KD and discuss the benefits that this yields for KD fidelity.

### 3. Explanation-Enhanced KD and Evaluating Distillation Fidelity

To increase KD fidelity, in Sec. 3.1 we introduce our proposed *explanation-enhanced KD* ( $e^2$ KD). Further, in Sec. 3.2, we present three desiderata that faithful KD should fulfill and why we expect  $e^2$ KD to be beneficial in the presented settings. Finally, in Sec. 3.3, we describe how to take advantage of  $e^2$ KD even without querying the teacher more than once per image when training the student.

**Notation.** For model  $M$  and input  $x$ , we denote the predicted class probabilities by  $p_M(x)$ , obtained using softmax  $\sigma(\cdot)$  over output logits  $z_M(x)$ , possibly scaled by temperature  $\tau$ . We denote the class with highest probability by  $\hat{y}_M$ .

#### 3.1. Explanation-Enhanced Knowledge Distillation

The logit-based knowledge distillation loss  $\mathcal{L}_{KD}$  which minimizes KL-Divergence  $D_{KL}$  between teacher  $T$  and student  $S$  output probabilities is given by

$$\begin{aligned} \mathcal{L}_{KD} &= \tau^2 D_{KL}(p_T(x; \tau) || p_S(x; \tau)) \\ &= -\tau^2 \sum_{j=1}^c \sigma_j \left( \frac{z_T}{\tau} \right) \log \sigma_j \left( \frac{z_S}{\tau} \right). \end{aligned} \quad (1)$$

In this work, we propose to leverage advances in model explanations for DNNs and explicitly include a term  $\mathcal{L}_{exp}$  that promotes explanation similarity to increase KD fidelity:

$$\mathcal{L} = \mathcal{L}_{KD} + \lambda \mathcal{L}_{exp}. \quad (2)$$

Specifically, we maximize the similarity between the models’ explanations, for the class  $\hat{y}_T$  predicted by the teacher:

$$\mathcal{L}_{exp} = 1 - \text{sim}(E(T, x, \hat{y}_T), E(S, x, \hat{y}_T)) . \quad (3)$$

Here,  $E(M, x, \hat{y}_T)$  denotes an explanation of model  $M$  for class  $\hat{y}_T$  and  $\text{sim}$  a similarity function; in particular, we rely on well-established explanation methods (e.g. GradCAM [37]) and use cosine similarity in our experiments.

**$e^2$ KD is model-agnostic.** Note that by computing the loss only across model outputs and explanations,  $e^2$ KD does not make any reference to architecture-specific details. In contrast to feature distillation approaches, which match specific blocks between teacher and student,  $e^2$ KD thus holds the potential to seamlessly work across different architectures without any need for adaptation. As we show in Sec. 4, this indeed seems to be the case, with  $e^2$ KD improving KD performance out of the box for a variety of model architectures, such as CNNs, B-cos CNNs, and even B-cos ViTs [6].

### 3.2. Evaluating Benefits of $e^2$ KD

In this section, we discuss three desiderata that faithful KD should fulfill and why we expect  $e^2$ KD to be beneficial.

#### 3.2.1 Desideratum 1: High Agreement with Teacher

First and foremost, faithful KD should ensure that the student classifies any given sample in the same way as the teacher, i.e., the student should have high agreement [40] with the teacher. For inputs  $\{x_i\}_{i=1}^N$  this is defined as:

$$\text{Agreement}(T, S) = \frac{1}{N} \sum_{i=1}^N \mathbb{1}_{\hat{y}_{i,T} = \hat{y}_{i,S}} . \quad (4)$$

While [40] found that more data points can improve the agreement, in practice, the original dataset that was used to train the teacher might be proprietary or prohibitively large (e.g. [31]). It is thus highly desirable to effectively distill knowledge *efficiently* with fewer data. As a proxy to evaluate the effectiveness of a given KD approach in such a setting, we propose to use a teacher trained on a large dataset (e.g. ImageNet [12]) and distill its knowledge to a student using as few as 50 images per class ( $\approx 4\%$  of the data) or even perform KD on images of an unrelated dataset.

Compared to standard supervised training, it has been argued that KD improves the student performance by providing more information (full logit distribution instead of binary labels). Similarly, by additionally providing the teachers’ explanations, we show that  $e^2$ KD boosts the performance even further, especially when fewer data is available to learn the same function as the teacher (Sec. 4.1).

#### 3.2.2 Desideratum 2: Learning the ‘Right’ Features

Despite achieving high accuracy, models often rely on spurious input features (are not “right for the right reasons” [35]), and can generalize better if guided to use the ‘right’ features via human annotations. This is particularly useful in the presence of distribution shifts [36]. Hence, faithful

distillation should ensure that student models also learn to use these ‘right’ features from a teacher that uses them.

To assess this, we use a binary classification dataset [36] in which the background is highly correlated with the class label in the training set, making it challenging for models to learn to use the actual class features for classification. We use a teacher that has explicitly been guided to focus on the actual class features and to ignore the background. Then, we evaluate the student’s accuracy and agreement with the teacher under distribution shift, i.e., at test time, we evaluate on images in which the class-background correlation is reversed. By providing additional spatial clues from the teachers’ explanations to the students, we find that  $e^2$ KD significantly improves performance over KD (Sec. 4.2).

### 3.2.3 Desideratum 3: Maintaining Interpretability

Further, note that the teacher models might be trained explicitly to exhibit certain desirable properties in their explanations [32], or do so as a result of a particular training paradigm [8] or the model architecture [6].

We propose two settings to test if such properties are transferred. First, we measure how well the students’ explanations reflect properties the teachers were explicitly trained for, i.e. how well they localize class-specific input features when using a teacher that has explicitly been guided to do so [32]. We find  $e^2$ KD to lend itself well to maintaining the interpretability of the teacher, as the explanations of students are explicitly optimized for this (Sec. 4.3.1).

Secondly, we perform a case study to assess whether KD can transfer priors that are not *learned*, but rather inherent to the model architecture. Specifically, the explanations of B-cos ViTs have been shown to be sensitive to image shifts [6], even when shifting by just a few pixels. To mitigate this, the authors of [6] proposed to use a short convolutional stem. Interestingly, in Sec. 4.3.2, we find that by learning from a CNN teacher under  $e^2$ KD, the explanations of a ViT student without convolutions also become largely invariant to image shifts, and exhibit similar patterns as the teacher.

### 3.3. $e^2$ KD with ‘Frozen’ Explanations

Especially in the ‘consistent teaching’ setup of [4], KD requires querying the teacher for every training step, as the input images are repeatedly augmented. To reduce the compute incurred by evaluating the teacher, the idea of using a ‘fixed teacher’ has been explored by prior logit-based KD approaches [15, 38, 44], where logits are pre-computed once at the start of training and used for all augmentations.

Analogously, we propose to use pre-computed explanations for images in the  $e^2$ KD framework. For this, we apply the same augmentations (e.g. cropping or flipping) to images and the teacher’s explanations during distillation. In Sec. 4.4, we show that  $e^2$ KD is robust to such ‘frozen’ ex-

planations, despite the fact that they of course only approximate the teacher’s explanations. As such, frozen explanations provide a trade-off between optimizing for explanation similarity and reducing the cost due to the teacher.

## 4. Results

In the following, we present our results. Specifically, in Sec. 4.1 we first compare various KD approaches in terms of accuracy and agreement on the ImageNet dataset as a function of the distillation dataset size. Thereafter, we present the results on learning the ‘right’ features from biased data in Sec. 4.2 and on maintaining the interpretability of the teacher models in Sec. 4.3. Lastly, in Sec. 4.4, we show that  $e^2$ KD can also yield significant benefits with approximate ‘frozen’ explanations (cf. Sec. 3.3).

Before turning to the results, however, in the following we first provide some general details with respect to our training setup and the explanations used for  $e^2$ KD.

**Training details.** In general, we follow the recent KD setup from [4], which has shown significant improvements for KD; results based on the setup followed by [9, 19, 45] can be found in the supplement. Unless specified otherwise, we use the AdamW optimizer [25] and, following [5], do not use weight decay for B-cos models. We use a cosine learning rate schedule with initial warmup for 5 epochs. For the teacher-student logit loss on multi-label VOC dataset, we use the logit loss following [43] instead of Eq. (1). For AT [45], CAT-KD [19], and ReviewKD [9], we follow the original implementation and use cross-entropy based on the ground truth labels instead of Eq. (1); for an adaptation to B-cos models, see supplement. For each method and setting, we report the results of the best hyperparameters (softmax temperature and the methods’ loss coefficients) as obtained on a separate validation set. Unless specified otherwise, we augment images via random horizontal flipping and random cropping with a final resize to  $224 \times 224$ . For full details, see supplement.

**Explanation methods.** For  $e^2$ KD, we use GradCAM [37] for standard models and B-cos explanations for B-cos models, optimizing the cosine similarity as per Eq. (3). For B-cos, we use the dynamic weights  $\mathbf{W}(\mathbf{x})$  as explanations [5].

### 4.1. $e^2$ KD Improves Learning from Limited Data

**Setup.** To test the robustness of  $e^2$ KD with respect to the dataset size (Sec. 3.2.1), we distill with 50 ( $\approx 4\%$ ) or 200 ( $\approx 16\%$ ) shots per class, as well as the full ImageNet training data; further, we also test without any access to ImageNet, by performing KD on the SUN397 [41], whilst still evaluating on ImageNet (and vice versa). We distill ResNet-34 [20] teachers into ResNet-18 students, both for standard and B-cos models; additionally, we use a B-cos DenseNet-169 [22] as a teacher to evaluate distillation across architectures.

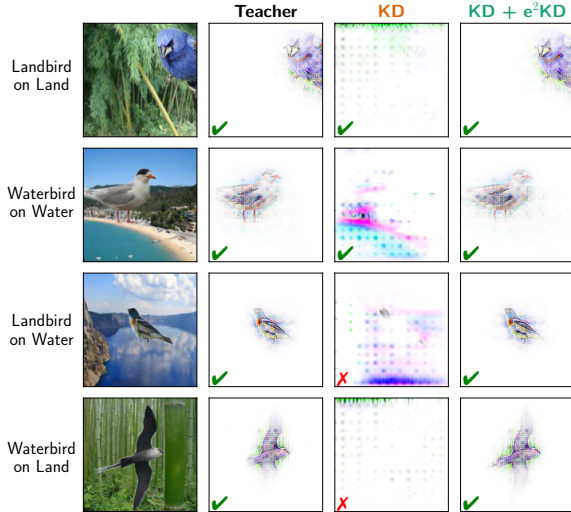


Figure 2. **Distillation on biased data.** We distill a B-cos ResNet-50 teacher (col. 2) to a B-cos ResNet-18 student with KD (col. 3) and  $e^2$ KD (col. 4). While for in-distribution data (rows 1+2) the different focus of the models (foreground/background) does not affect the models’ predictions (correct predictions marked by ✓), it results in wrong predictions under distribution shift (rows 3+4, incorrect predictions marked by ✗).

For reference, we also provide results as obtained via attention transfer (AT) [45], CAT-KD [19], and ReviewKD [9].

**Results.** In Tabs. 1 and 2, we show that  $e^2$ KD can significantly improve KD in terms of top-1 accuracy as well as top-1 agreement with the teacher on ImageNet. We observe particularly large gains for small distillation dataset sizes. E.g., accuracy and agreement for conventional models on 50 shots improve by 5.1 (B-cos: 8.6) and 6.2 (B-cos: 10.0) p.p. respectively. In Tab. 5, we show that  $e^2$ KD also provides significant gains in the ‘data-free’ setting [4], improving the accuracy and agreement of the student by 4.9 and 5.4 p.p. respectively, despite computing the explanations on an unrelated dataset (i.e. SUN→ImageNet, right). Similar gains can be observed when using ImageNet images to distill a teacher trained on SUN (i.e. ImageNet→SUN, left).

#### 4.2. $e^2$ KD Improves Learning the ‘Right’ Features

**Setup.** To assess whether the students learn to use the same input features as the teacher (Sec. 3.2.2), we use the Waterbirds-100 dataset [36], a binary classification task between land- and waterbirds, in which birds are highly correlated with the image backgrounds during training. As teachers, we use pre-trained ResNet-50 models from [32], which were guided to use the bird features instead of the background; as in Sec. 4.1, we use conventional and B-cos models and provide results obtained via prior work for reference.

**Results.** In Fig. 4, we present our results on the Waterbirds dataset for standard models. Specifically, we evaluate

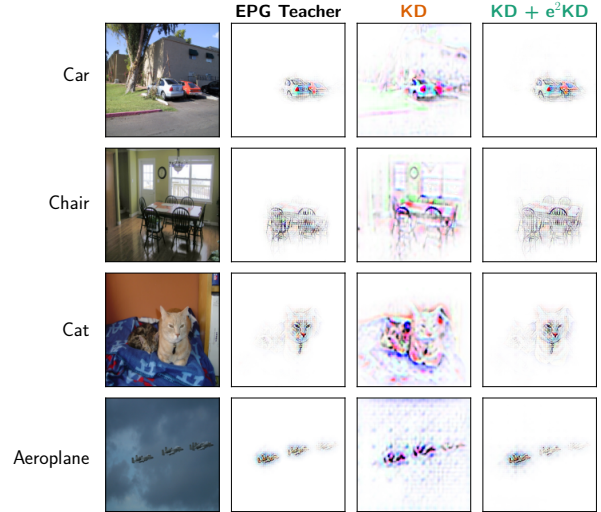


Figure 3. **Maintaining focused explanations.** We distill a B-cos ResNet-50 teacher that has been trained with the EPG loss to not focus on confounding input features (col. 2), to a B-cos ResNet-18 student with KD (col. 3) and  $e^2$ KD (col. 4). We see that the explanations for  $e^2$ KD are significantly closer to the teacher’s (and hence more human-aligned). Samples are drawn from the VOC test set, with all models correctly classifying the shown samples.

the accuracy and student-teacher agreement of each method on object-background combinations not seen during training (i.e. ‘Waterbirds on Land’ and ‘Landbirds on Water’) to assess how well the students learnt from the teacher to rely on the ‘right’ input features (i.e. the birds).

In light of the findings by [4] that long teaching schedules and strong data augmentations help, we do so for three settings<sup>2</sup>: (1) for 700 epochs, (2) with add. mixup [46], as well as (3) for training 5x longer (‘patient teaching’).

Across settings, we find that  $e^2$ KD consistently and significantly improves the performance of KD both in terms of accuracy and agreement. Despite its simplicity, it compares favourably to prior work in terms of accuracy and agreement, indicating that  $e^2$ KD indeed helps improving KD fidelity. For quantitative results obtained with B-cos models, see Fig. 1 (center) and supplement. We also find clear qualitative improvements in the model’s ability to focus on the ‘right’ features, see Fig. 2.

Further, consistent with [4], we find mixup augmentation and longer training schedules to also significantly improve agreement. This provides additional evidence for the hypothesis put forward by [4] that KD *could* be sufficient for function matching if performed for long enough. As such, and given the simplicity of the dataset, the low resource requirements, and a clear target (100% agreement on unseen

<sup>2</sup>Compared to ImageNet, the small size of the Waterbirds-100 dataset allows for reproducing the ‘patient teaching’ results with limited compute.

Standard Models Teacher ResNet-34 Accuracy 73.3%	50 Shots		200 Shots		Full data	
	Accuracy	Agreement	Accuracy	Agreement	Accuracy	Agreement
Baseline ResNet-18	23.3	24.8	47.0	50.2	69.8	76.8
AT [45]	38.3	41.1	54.7	59.0	69.7	74.9
ReviewKD [9]	51.2	55.6	63.0	69.0	71.4	80.0
CAT-KD [19]	32.1	34.5	55.7	60.7	70.9	78.7
KD [4, 21]	49.8	55.5	63.1	71.9	<b>71.8</b>	81.2
+ e <sup>2</sup> KD (GradCAM)	<b>54.9 (+ 5.1)</b>	<b>61.7 (+ 6.2)</b>	<b>64.1 (+ 1.0)</b>	<b>73.2 (+ 1.3)</b>	<b>71.8 (+ 0.0)</b>	<b>81.6 (+ 0.4)</b>

Table 1. **KD on ImageNet for standard models.** For a ResNet-34 teacher and a ResNet-18 student, we show the accuracy and agreement of various KD approaches for three different distillation dataset sizes. We observe that across all settings e<sup>2</sup>KD yields significant top-1 accuracy gains over vanilla KD, while remaining competitive with prior work. Crucially, e<sup>2</sup>KD also exhibits the highest degree of distillation fidelity as measured by the top-1 agreement with the teacher. Similar results are also observed for B-cos models, see Tab. 2.

B-cos Models Teacher ResNet-34 Accuracy 72.3%	50 Shots		200 Shots		Full data	
	Accuracy	Agreement	Accuracy	Agreement	Accuracy	Agreement
Baseline ResNet-18	32.6	35.1	53.9	59.4	68.7	76.9
AT [45]	41.9	45.6	57.2	63.7	69.0	77.2
ReviewKD [9]	47.5	53.2	54.1	60.8	57.0	64.6
CAT-KD [19]	53.1	59.8	58.6	66.4	63.9	73.7
KD [4, 21]	35.3	38.4	56.5	62.9	70.3	79.9
+ e <sup>2</sup> KD (B-cos)	<b>43.9 (+ 8.6)</b>	<b>48.4 (+10.0)</b>	<b>58.8 (+ 2.3)</b>	<b>66.0 (+ 3.1)</b>	<b>70.6 (+ 0.3)</b>	<b>80.3 (+ 0.4)</b>

Table 2. **KD on ImageNet for B-cos models.** For a B-cos ResNet-34 teacher and a B-cos ResNet-18 student, we show the accuracy and agreement of various KD approaches for three different distillation dataset sizes. We observe that across all settings e<sup>2</sup>KD yields significant accuracy and agreement gains over vanilla KD, whilst also remaining competitive with prior work.

B-cos Models Teacher DenseNet-169 Accuracy 75.2%	50 Shots		200 Shots		Full data	
	Accuracy	Agreement	Accuracy	Agreement	Accuracy	Agreement
Baseline ResNet-18	32.6	34.5	53.9	58.4	68.7	75.5
KD [4, 21]	37.3	40.2	51.3	55.6	71.2	78.8
+ e <sup>2</sup> KD (B-cos)	<b>45.4 (+ 8.1)</b>	<b>49.0 (+ 8.8)</b>	<b>55.7 (+ 4.4)</b>	<b>60.7 (+ 5.1)</b>	<b>71.9 (+ 0.7)</b>	<b>79.8 (+ 1.0)</b>
✳ KD	33.4	35.7	50.4	54.5	68.7	75.2
✳ + e <sup>2</sup> KD (B-cos)	<b>38.7 (+ 5.3)</b>	<b>41.7 (+ 6.0)</b>	<b>53.6 (+ 3.2)</b>	<b>58.3 (+ 3.8)</b>	<b>69.5 (+ 0.8)</b>	<b>76.4 (+ 1.2)</b>

Table 3. **KD on ImageNet for B-cos models for a DenseNet-169 teacher and with ‘frozen’ (✳) explanations and logits.** Similar to the results in Tab. 2, we find that e<sup>2</sup>KD adds significant gains to ‘vanilla’ KD across dataset sizes (50 Shots, 200 Shots, full data). Given that e<sup>2</sup>KD does not rely on matching specific blocks between architectures (cf. [9, 45]), it seamlessly generalizes across architectures. Further, e<sup>2</sup>KD can also be performed with ‘frozen’ (✳) explanations by augmenting images and pre-computed explanations jointly (Sec. 3.3).

combinations), we believe the waterbirds dataset to constitute a great benchmark for future research on KD fidelity.

### 4.3. e<sup>2</sup>KD Improves the Student’s Interpretability

In this section, we show results on maintaining the teacher’s interpretability (cf. Sec. 3.2.3). In particular, we show that e<sup>2</sup>KD naturally lends itself to distilling localization properties into the student that the teacher was trained for (Sec. 4.3.1) and that even architectural priors of a CNN teacher can be transferred to a ViT student (Sec. 4.3.2).

#### 4.3.1 Maintaining Focused Explanations

**Setup.** To assess whether the students learn to give similar explanations as the teachers, we distill B-cos ResNet-50 teachers into B-cos ResNet-18 students on PASCAL VOC [13] in a multi-label classification setting. Specifically, we use two different teachers: one with a high EPG (EPG Teacher), and one with a high IoU score (IoU Teacher). To quantify the students’ focus, we measure the EPG and IoU scores [32] of the explanations with respect to the dataset’s bounding box annotations in a multi-label classification setting. As these teachers are trained explicitly to exhibit cer-

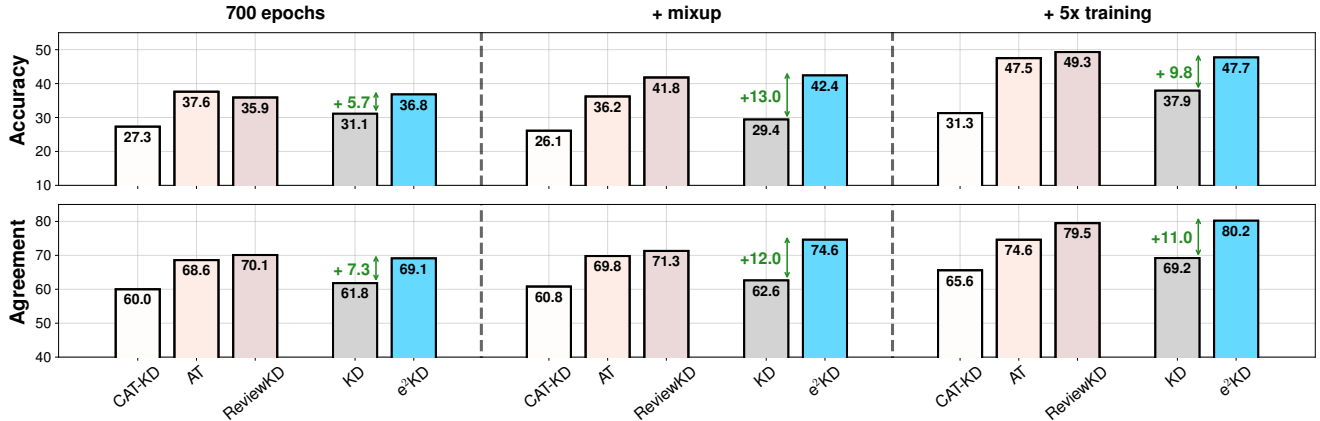


Figure 4. **KD on out-of-distribution data for standard models on Waterbirds-100.** We show the accuracy (top) and agreement (bottom) when distilling from a ResNet-50 teacher to a ResNet-18 student with various KD approaches. Following [4], we additionally evaluate the effectiveness of adding mixup (col. 2) and, additionally, long teaching (col. 3). We find that our proposed e<sup>2</sup>KD provides significant benefits in both accuracy and agreement over vanilla KD, and is further enhanced by the use of long teaching and mixup. We show the performance of prior work for reference, and find that e<sup>2</sup>KD performs competitively. For results on B-cos models, please see the supplement.

tain properties in their explanations, a *faithfully distilled* student should optimally exhibit the same properties. **Results.** As we show in Tab. 4, the explanations of an e<sup>2</sup>KD student indeed more closely mirror those of the teacher than a student trained via vanilla KD: e<sup>2</sup>KD students exhibit significantly higher EPG when distilled from the EPG teacher (EPG: 71.1 vs. 60.3) and vice versa (IoU: 45.7 vs. 24.8). In contrast, ‘vanilla’ KD students show only minor differences (EPG: 60.1 vs. 58.9; IoU: 35.7 vs. 31.6). Fig. 3 shows that these improvements are also reflected qualitatively, with the e<sup>2</sup>KD students reflecting the teacher’s focus much more faithfully in their explanations.

While this might be expected as e<sup>2</sup>KD explicitly optimizes for explanation similarity, we would like to highlight that this not only ensures that the desired properties of the teachers are better represented in the student model, but also significantly improves the students’ performance (e.g., F1: 60.1 → 67.6 for the EPG teacher). As such, we find e<sup>2</sup>KD to be an easy-to-use and effective addition to vanilla KD for improving both interpretability as well as task performance.

### 4.3.2 Distilling Architectural Priors

**Setup.** To test whether students learn architectural priors of the models, we evaluate whether a B-cos ViT<sub>Tiny</sub> student model can learn to give explanations that are similar to those of a pretrained CNN (B-cos DenseNet-169) teacher model; for this, we again use the ImageNet dataset.

**Results.** In line with the results of the preceding sections, we find (Fig. 5, left) that e<sup>2</sup>KD significantly improves the accuracy of the ViT student model (64.8 → 66.3), as well as the agreement with the teacher (70.1 → 71.8).

Interestingly, we find that the ViT student’s explanations

seem to become similarly robust to image shifts as those of the teacher (Fig. 5, center and right). Specifically, note that the image tokenization of the ViT model using vanilla KD (extracting non-overlapping patches of size 16 × 16) induces a periodicity of 16 with respect to image shifts  $T$ , see, e.g., Fig. 5 (center, yellow curve): here, we plot the cosine similarity of the explanations<sup>3</sup> at various shifts with respect to the explanation given for the original, unshifted image ( $T=0$ ). In contrast, due to smaller strides ( $\text{stride} \in \{1, 2\}$  for any layer) and overlapping convolutional kernels, the CNN teacher model is inherently more robust to image shifts, see Fig. 5 (center, purple curve), exhibiting a periodicity of 4. A ViT student trained via e<sup>2</sup>KD learns to mimic the behaviour of the teacher (see Fig. 5, center, blue curve) and exhibits the same periodicity, indicating that e<sup>2</sup>KD indeed helps the student learn a function more similar to the teacher. Importantly, this also helps significantly improving the explanations of the ViT model, see Fig. 5 (right). In particular, we show the explanations for images at a diagonal shift of 0 and 8 pixels. As can be seen, the explanations become more robust to such shifts and more easily interpretable, thus maintaining the utility of the explanations of the teacher.

Notably, our results indicate that it might be possible to instill desired properties into a DNN model even beyond knowledge distillation. E.g., note that the frozen explanations (see also Sec. 4.4) do not exhibit the CNN’s periodicity, as *by design* they maintain consistent augmentations across shifts and crops. Based on our observations for the ViTs, we thus expect a student trained on frozen explanations to become almost *fully shift-equivariant*, which is indeed the case (see Fig. 5, center, red curve, ViT \* e<sup>2</sup>KD).

<sup>3</sup>We compute the similarity of the intersecting area of the explanations.

	EPG Teacher			IoU Teacher		
	EPG	IoU	F1	EPG	IoU	F1
Teacher ResNet-50	75.7	21.3	72.5	65.0	49.7	72.8
Baseline ResNet-18	50.0	29.0	58.0	50.0	29.0	58.0
KD [43]	60.1	31.6	60.1	58.9	35.7	62.7
+ $e^2$ KD (B-cos)	<b>71.1</b>	24.8	<b>67.6</b>	60.3	<b>45.7</b>	<b>64.8</b>

Table 4.  $e^2$ KD results on VOC. We compare KD and  $e^2$ KD when distilling from a teacher guided [32] to either optimize for EPG (left) or IoU (right). Explanations of the  $e^2$ KD student better align with those of the teacher, as evidenced by significantly higher EPG (IoU) scores when distilled from the EPG (IoU) teacher.  $e^2$ KD students also achieve higher accuracy (F1).

	IMN→SUN		SUN→IMN	
	Acc.	Agr.	Acc.	Agr.
Teacher DenseNet-169	60.5	-	75.2	-
Baseline ResNet-18	57.7	67.9	68.7	75.5
KD [4, 21]	53.5	65.0	14.9	16.7
+ $e^2$ KD (B-cos)	<b>54.9</b>	<b>67.7</b>	<b>19.8</b>	<b>22.1</b>

Table 5. KD in data-free setting. We distill a B-cos DenseNet-169 teacher model, left: trained on the SUN [41] dataset using ImageNet (IMN→SUN), and right: trained on ImageNet using SUN (SUN→IMN). In both cases, we see that the B-cos ResNet-18 student distilled with  $e^2$ KD achieves significantly higher accuracy and agreement scores than student trained via vanilla KD.

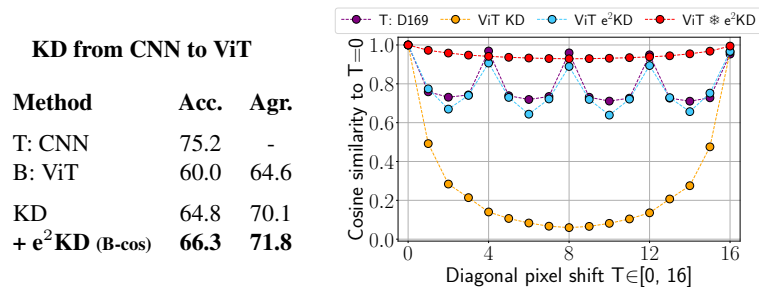


Figure 5. **Distilling inductive biases from CNN to ViT.** We distill a B-cos DenseNet-169 teacher to a B-cos ViT<sub>Tiny</sub>. **Left:** We find  $e^2$ KD to yield significant gains in both accuracy and agreement. **Center:** Cosine similarity of explanations for shifted images w.r.t. the unshifted image ( $T=0$ ). We find that under  $e^2$ KD (blue) the ViT student learns to mimic the shift periodicity of the teacher (purple), despite the inherent periodicity of 16 of the ViT architecture (seen for vanilla KD, yellow). Notably,  $e^2$ KD with frozen explanations yields shift-equivariant students (red), see also Sec. 4.3.2. **Right:**  $e^2$ KD significantly improves the explanations of the ViT model, thus maintaining the utility of the explanations of the teacher model. While the explanations for KD change significantly under shift (subcol. 3), for  $e^2$ KD (subcol. 4), as with the CNN teacher (subcol. 2), the explanations remain consistent. For more qualitative samples, see supplement.

#### 4.4. $e^2$ KD with Frozen Explanations

In the previous sections, we have seen that  $e^2$ KD is a robust approach that provides consistent gains even when only limited data is available (see Sec. 4.1) and works across different architectures (e.g., DenseNet→ResNet or DenseNet→ViT, see Secs. 4.1 and 4.3.2). In the following, we show that  $e^2$ KD even works when only ‘approximate’ explanations for the teacher are available (cf. Sec. 3.3).

**Setup.** To test the robustness of  $e^2$ KD when using frozen explanations, we distill from a B-cos DenseNet-169 teacher to a B-cos ResNet-18 student using pre-computed, frozen explanations on the ImageNet dataset. We also evaluate across varying dataset sizes, as in Sec. 4.1.

**Results.** Tab. 3 (bottom) shows that  $e^2$ KD with frozen explanations is effective for improving both the accuracy and agreement over KD with frozen logits across dataset sizes (e.g. accuracy: 33.4→38.7 for 50 shots). Furthermore,  $e^2$ KD with frozen explanations also outperforms vanilla KD under both metrics when using limited data (e.g. accuracy: 37.3→38.7 for 50 shots). As such, a frozen teacher con-

stitutes a more cost-effective alternative for obtaining the benefits of  $e^2$ KD, whilst also highlighting its robustness to using ‘approximate’ explanations.

## 5. Conclusion

We proposed a simple approach to improve knowledge distillation (KD) by explicitly optimizing for the explanation similarity between the teacher and the student, and showed its effectiveness in distilling the teacher’s properties under multiple settings. Specifically,  $e^2$ KD helps the student (1) achieve competitive and often higher accuracy and agreement than vanilla KD, (2) learn to be ‘right for the right reasons’, and (3) learn to give similar explanations as the teacher, e.g. even when distilling from a CNN teacher to a ViT student. Finally, we showed that  $e^2$ KD is robust in the presence of limited data, approximate explanations, and across model architectures. In short, we find  $e^2$ KD to be a simple but versatile addition to KD that allows for more faithfully distilling a teacher’s knowledge into a student while also maintaining competitive task performance.

## References

- [1] R. Alharbi, M. N. Vu, and M. T. Thai. Learning Interpretation with Explainable Knowledge Distillation. In *2021 IEEE International Conference on Big Data (Big Data)*, pages 705–714, Los Alamitos, CA, USA, 2021. IEEE Computer Society. **2**
- [2] Sebastian Bach, Alexander Binder, Grégoire Montavon, Frederick Klauschen, Klaus-Robert Müller, and Wojciech Samek. On Pixel-wise Explanations for Non-linear Classifier Decisions by Layer-wise Relevance Propagation. *PLoS one*, 10(7):e0130140, 2015. **2**
- [3] Gagan Bansal, Besmira Nushi, Ece Kamar, Daniel S Weld, Walter S Lasecki, and Eric Horvitz. Updates in Human-AI Teams: Understanding and Addressing the Performance/Compatibility Tradeoff. In *AAAI*, pages 2429–2437, 2019. **1**
- [4] Lucas Beyer, Xiaohua Zhai, Amélie Royer, Larisa Markeeva, Rohan Anil, and Alexander Kolesnikov. Knowledge Distillation: A Good Teacher Is Patient and Consistent. In *CVPR*, 2022. **1, 2, 4, 5, 6, 7, 8, 17, 20**
- [5] Moritz Böhle, Mario Fritz, and Bernt Schiele. B-cos Networks: Alignment Is All We Need for Interpretability. In *CVPR*, 2022. **2, 3, 4, 12, 20**
- [6] Moritz Böhle, Navdeepsingh Singh, Mario Fritz, and Bernt Schiele. B-cos Alignment for Inherently Interpretable CNNs and Vision Transformers. *IEEE Transactions on Pattern Analysis and Machine Intelligence*, 2024. **3, 4, 12, 20, 21**
- [7] Andy Brock, Soham De, Samuel L Smith, and Karen Simonyan. High-Performance Large-Scale Image Recognition Without Normalization. In *Proceedings of the 38th International Conference on Machine Learning*, pages 1059–1071. PMLR, 2021. **20**
- [8] Mathilde Caron, Hugo Touvron, Ishan Misra, Hervé Jégou, Julien Mairal, Piotr Bojanowski, and Armand Joulin. Emerging Properties in Self-Supervised Vision Transformers. In *ICCV*, pages 9650–9660, 2021. **4**
- [9] Pengguang Chen, Shu Liu, Hengshuang Zhao, and Jiaya Jia. Distilling Knowledge via Knowledge Review. In *CVPR*, 2021. **2, 4, 5, 6, 17**
- [10] Council of the European Union. Proposal for a Regulation of the European Parliament and of the Council Laying Down Harmonised Rules on Artificial Intelligence (Artificial Intelligence Act) and Amending Certain Union Legislative Acts. <https://eur-lex.europa.eu/legal-content/EN/TXT/?uri=celex:52021PC0206>, 2021. Accessed: 2023-11-15. **1**
- [11] Ekin Dogus Cubuk, Barret Zoph, Jon Shlens, and Quoc Le. RandAugment: Practical Automated Data Augmentation with a Reduced Search Space. In *Advances in Neural Information Processing Systems*, pages 18613–18624. Curran Associates, Inc., 2020. **20**
- [12] Jia Deng, Wei Dong, Richard Socher, Li-Jia Li, Kai Li, and Li Fei-Fei. ImageNet: A Large-Scale Hierarchical Image Database. In *CVPR*, Ieee, 2009. **2, 3, 20**
- [13] Mark Everingham, Luc Van Gool, Christopher KI Williams, John Winn, and Andrew Zisserman. The Pascal Visual Object Classes (VOC) Challenge. *IJCV*, 88, 2009. **2, 6**
- [14] M. Everingham, L. Van Gool, C. K. I. Williams, J. Winn, and A. Zisserman. The PASCAL Visual Object Classes Challenge 2012 (VOC2012) Results. <http://www.pascal-network.org/challenges/VOC/voc2012/workshop/index.html>, 2012. **21**
- [15] Fartash Faghri, Hadi Pouransari, Sachin Mehta, Mehrdad Farajtabar, Ali Farhadi, Mohammad Rastegari, and Oncel Tuzel. Reinforce Data, Multiply Impact: Improved Model Accuracy and Robustness with Dataset Reinforcement. In *ICCV*, 2023. **2, 4**
- [16] William Falcon and The PyTorch Lightning team. PyTorch Lightning, 2019. **20**
- [17] Yuyang Gao, Tong Steven Sun, Guangji Bai, Siyi Gu, Sungsoo Ray Hong, and Zhao Liang. RES: A Robust Framework for Guiding Visual Explanation. In *KDD*, pages 432–442, 2022. **3**
- [18] Yuyang Gao, Tong Steven Sun, Liang Zhao, and Sungsoo Ray Hong. Aligning Eyes between Humans and Deep Neural Network through Interactive Attention Alignment. *Proceedings of the ACM on Human-Computer Interaction*, 6(CSCW2):1–28, 2022. **3**
- [19] Ziyao Guo, Haonan Yan, Hui Li, and Xiaodong Lin. Class Attention Transfer Based Knowledge Distillation. In *CVPR*, 2023. **2, 4, 5, 6, 17**
- [20] Kaiming He, Xiangyu Zhang, Shaoqing Ren, and Jian Sun. Deep Residual Learning for Image Recognition. In *CVPR*, pages 770–778, 2016. **4, 21**
- [21] Geoffrey Hinton, Oriol Vinyals, and Jeffrey Dean. Distilling the Knowledge in a Neural Network. In *NeurIPS*, 2015. **1, 2, 6, 8, 17**
- [22] Gao Huang, Zhuang Liu, Laurens Van Der Maaten, and Kilian Q Weinberger. Densely Connected Convolutional Networks. In *CVPR*, pages 4700–4708, 2017. **4**
- [23] Diederik P Kingma and Jimmy Ba. Adam: A Method for Stochastic Optimization. In *ICLR*, 2015. **20**
- [24] Ilya Loshchilov and Frank Hutter. SGDR: Stochastic gradient descent with warm restarts. In *International Conference on Learning Representations*, 2017. **20**
- [25] Ilya Loshchilov and Frank Hutter. Decoupled Weight Decay Regularization. In *ICLR*, 2019. **4**
- [26] TorchVision maintainers and contributors. TorchVision: PyTorch’s Computer Vision library. <https://github.com/pytorch/vision>, 2016. **20**
- [27] Yoshitomo Matsubara. torchdistill: A Modular, Configuration-Driven Framework for Knowledge Distillation. In *International Workshop on Reproducible Research in Pattern Recognition*, pages 24–44. Springer, 2021. **17**
- [28] Utkarsh Ojha, Yuheng Li, and Yong Jae Lee. What Knowledge gets Distilled in Knowledge Distillation? *arXiv preprint arXiv:2205.16004*, 2022. **2**
- [29] Adam Paszke, Sam Gross, Francisco Massa, Adam Lerer, James Bradbury, Gregory Chanan, Trevor Killeen, Zeming Lin, Natalia Gimelshein, Luca Antiga, Alban Desmaison, Andreas Kopf, Edward Yang, Zachary DeVito, Martin Raison, Alykhan Tejani, Sasank Chilamkurthy, Benoit Steiner, Lu Fang, Junjie Bai, and Soumith Chintala. PyTorch: An

- Imperative Style, High-Performance Deep Learning Library. In *NeurIPS*, 2019. [20](#)
- [30] Suzanne Petryk, Lisa Dunlap, Keyan Nasseri, Joseph Gonzalez, Trevor Darrell, and Anna Rohrbach. On Guiding Visual Attention with Language Specification. *CVPR*, 2022. [2](#), [3](#), [12](#), [18](#), [21](#)
- [31] Alec Radford, Jong Wook Kim, Chris Hallacy, Aditya Ramesh, Gabriel Goh, Sandhini Agarwal, Girish Sastry, Amanda Askell, Pamela Mishkin, Jack Clark, Gretchen Krueger, and Ilya Sutskever. Learning Transferable Visual Models from Natural Language Supervision. In *ICML*, pages 8748–8763, 2021. [3](#)
- [32] Sukrut Rao, Moritz Böhle, Amin Parchami-Araghi, and Bernt Schiele. Studying How to Efficiently and Effectively Guide Models with Explanations. In *ICCV*, 2023. [3](#), [4](#), [5](#), [6](#), [8](#), [21](#)
- [33] Marco Tulio Ribeiro, Sameer Singh, and Carlos Guestrin. “Why Should I Trust You?” Explaining the Predictions of Any Classifier. In *KDD*, pages 1135–1144, 2016. [2](#)
- [34] Adriana Romero, Nicolas Ballas, Samira Ebrahimi Kahou, Antoine Chassang, Carlo Gatta, and Yoshua Bengio. FitNets: Hints for Thin Deep Nets. In *ICLR*, 2015. [2](#)
- [35] Andrew Slavin Ross, Michael C Hughes, and Finale Doshi-Velez. Right for the Right Reasons: Training Differentiable Models by Constraining their Explanations. In *IJCAI*, 2017. [1](#), [3](#)
- [36] Shiori Sagawa, Pang Wei Koh, Tatsunori B Hashimoto, and Percy Liang. Distributionally Robust Neural Networks for Group Shifts: On the Importance of Regularization for Worst-Case Generalization. In *ICLR*, 2020. [2](#), [3](#), [4](#), [5](#), [12](#), [18](#), [21](#)
- [37] Ramprasaath R. Selvaraju, Michael Cogswell, Abhishek Das, Ramakrishna Vedantam, Devi Parikh, and Dhruv Batra. Grad-CAM: Visual Explanations from Deep Networks via Gradient-Based Localization. In *ICCV*, 2017. [2](#), [3](#), [4](#), [12](#)
- [38] Zhiqiang Shen and Eric Xing. A Fast Knowledge Distillation Framework for Visual Recognition. In *ECCV*, pages 673–690, Cham, 2022. Springer Nature Switzerland. [2](#), [4](#)
- [39] Suraj Srinivas and François Fleuret. Knowledge Transfer with Jacobian Matching. In *ICML*, 2018. [2](#)
- [40] Samuel Stanton, Pavel Izmailov, Polina Kirichenko, Alexander A Alemi, and Andrew G Wilson. Does Knowledge Distillation Really Work? In *NeurIPS*. Curran Associates, Inc., 2021. [1](#), [2](#), [3](#)
- [41] J. Xiao, J. Hays, K. A. Ehinger, A. Oliva, and A. Torralba. SUN database: Large-Scale Scene Recognition from Abbey to Zoo. In *CVPR*, pages 3485–3492, 2010. [4](#), [8](#)
- [42] Sijie Yan, Yuanjun Xiong, Kaustav Kundu, Shuo Yang, Siqi Deng, Meng Wang, Wei Xia, and Stefano Soatto. Positive-congruent Training: Towards Regression-free Model Updates. In *CVPR*, pages 14299–14308, 2021. [1](#)
- [43] Penghui Yang, Ming-Kun Xie, Chen-Chen Zong, Lei Feng, Gang Niu, Masashi Sugiyama, and Sheng-Jun Huang. Multi-Label Knowledge Distillation. In *ICCV*, 2023. [4](#), [8](#), [21](#)
- [44] Sangdoon Yun, Seong Joon Oh, Byeongho Heo, Dongyoon Han, Junsuk Choe, and Sanghyuk Chun. Re-Labeling ImageNet: From Single to Multi-Labels, From Global to Localized Labels. In *CVPR*, pages 2340–2350, 2021. [2](#), [4](#)
- [45] Sergey Zagoruyko and Nikos Komodakis. Paying More Attention to Attention: Improving the Performance of Convolutional Neural Networks via Attention Transfer. In *ICLR*, 2017. [2](#), [4](#), [5](#), [6](#), [17](#)
- [46] Hongyi Zhang, Moustapha Cisse, Yann N. Dauphin, and David Lopez-Paz. mixup: Beyond Empirical Risk Minimization. In *ICLR*, 2018. [5](#)
- [47] Borui Zhao, Quan Cui, Renjie Song, Yiyu Qiu, and Jiajun Liang. Decoupled knowledge distillation. In *CVPR*, 2022. [2](#)
- [48] B. Zhou, A. Khosla, A. Lapedriza, A. Oliva, and A. Torralba. Learning Deep Features for Discriminative Localization. In *CVPR*, 2016. [2](#)

# Good Teachers Explain: Explanation-Enhanced Knowledge Distillation

## Supplementary Material

### Table of Contents

In this supplement to our work on explanation-enhanced knowledge distillation ( $e^2$ KD), we provide:

**(A) Additional Qualitative Results** ..... **12**

In this section, we provide additional qualitative results for each evaluation setting. Specifically, we show qualitative results of the model explanations of standard models (GradCAM) and B-cos models (B-cos explanations) for KD and  $e^2$ KD for the following:

- (A.1)** Learning the ‘right’ features (Waterbirds-100).
- (A.2)** Maintaining focused explanations (PASCAL VOC).
- (A.3)** Distilling architectural priors (CNN→ViT on ImageNet).

**(B) Additional Quantitative Results** ..... **17**

In this section, we provide additional quantitative results:

- (B.1)** Reproducing previously reported results for prior work on ImageNet.
- (B.2)** In-distribution and out-of-distribution results for B-cos and conventional models on Waterbirds.

**(C) Implementation Details** ..... **20**

In this section, we provide implementation details, including the setup used in each experiment and the procedure followed to adapt prior work to B-cos models. Code will be made available on publication.

- (C.1)** Training details.
- (C.2)** Adaptation of prior work to B-cos networks.

## A. Additional Qualitative Results

### A.1. Learning the ‘Right’ Features

In this section we provide qualitative results on the Waterbirds-100 dataset [30, 36]. We show GradCAM explanations [37] for standard models and B-cos explanations for B-cos models [5, 6]. In Fig. A1, we show explanations for in-distribution (i.e. ‘Landbird on Land’ and ‘Waterbird on Water’) test samples, and in Fig. A2 we show them for out-of-distribution samples (i.e. ‘Landbird on Water’ and ‘Waterbird on Land’). Corresponding quantitative results can be found in Sec. B.2.

From Fig. A1, we observe that the explanations of the teacher and vanilla KD student may significantly differ (for both standard and B-cos models): while the teacher is focusing on the bird, the student may use spuriously correlated input-features (i.e. background). We observe that  $e^2$ KD is successfully promoting explanation similarity and keeping the student ‘right for right reasons’. While in Fig. A1 (i.e. in-distribution data) all models correctly classify the samples despite the difference in their focus, in Fig. A2 (i.e. out-of-distribution) we observe that the student trained with  $e^2$ KD is able to arrive at the correct prediction, whereas the vanilla KD student wrongly classifies the samples based on the background type.

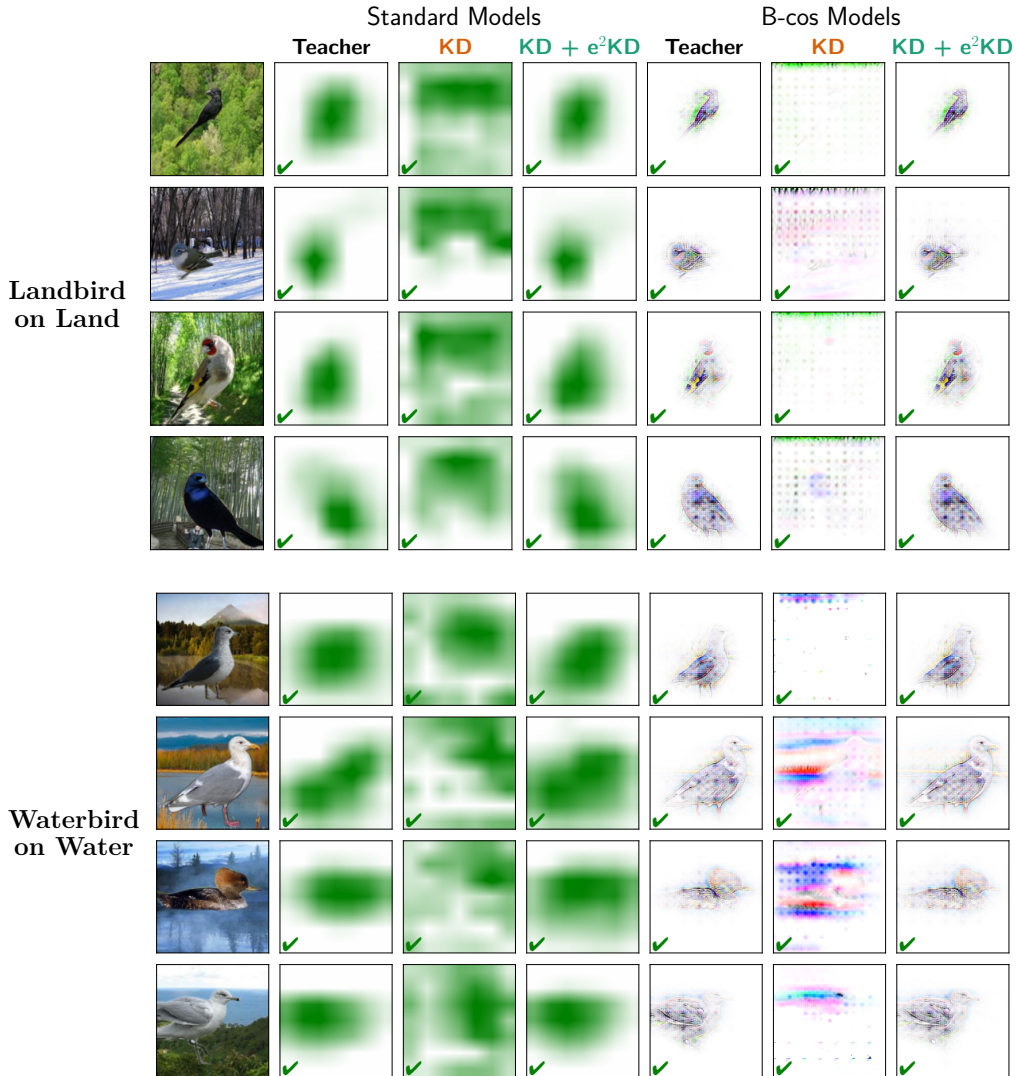


Figure A1. **In-distribution samples for distillation on biased data using the Waterbirds-100 dataset.** We show explanations for both standard models (cols. 2-4) and B-cos models (cols. 5-7), given both in-distribution groups: ‘Landbird on Land’ (**top half**) and ‘Waterbird on Water’ (**bottom half**). We find that  $e^2$ KD approach (col. 4 and 7) is effective in preserving the teacher’s focus (col. 2 and 5) to the bird instead of the background as opposed to vanilla KD (col. 3 and 6). Correct and incorrect predictions marked by ✓ and ✗ respectively.

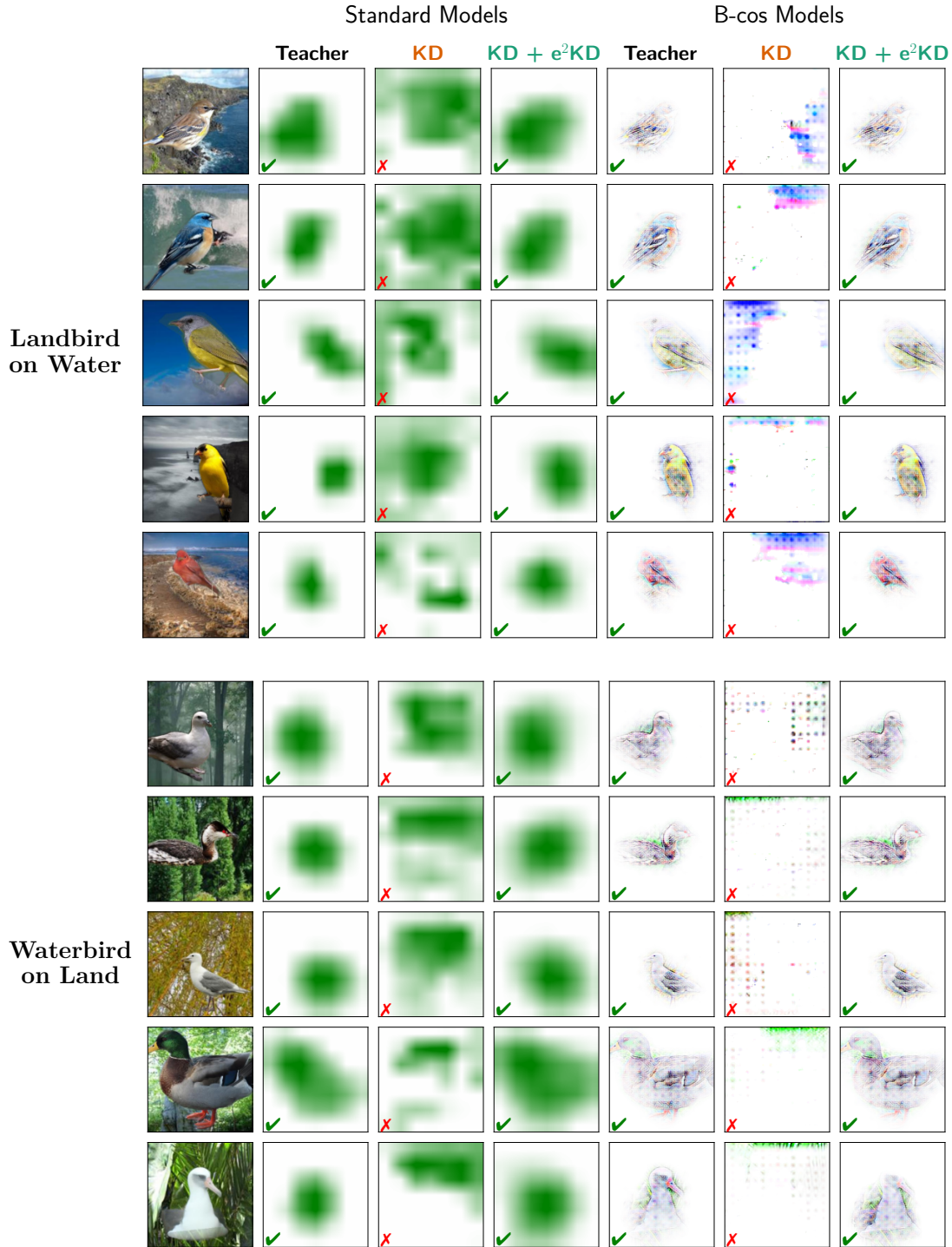


Figure A2. **Out-of-distribution samples for distillation on biased data using the Waterbirds-100 dataset.** We show explanations for standard (cols. 2-4) and B-cos models (cols. 5-7), for the out-of-distribution groups ‘Landbird on Water’ (top half) and ‘Waterbird on Land’ (bottom half). e<sup>2</sup>KD (col. 4 and 7) is effective in preserving the teacher’s focus (col. 2 and 5), leading to higher robustness to distribution shifts than when training students via vanilla KD. Correct and incorrect predictions marked by ✓ and ✗ respectively.

## A.2. Maintaining Focused Explanations

In this section we provide additional qualitative examples for experiments on PASCAL VOC (see Sec. 4.3.1). We provide samples for all of the 20 classes in the PASCAL VOC dataset (every row in Figs. A3 and A4). Across all classes we observe that the student trained with  $e^2$ KD maintains focused explanations on the class-specific input-features, whereas the student trained with vanilla KD may often focus on the background.

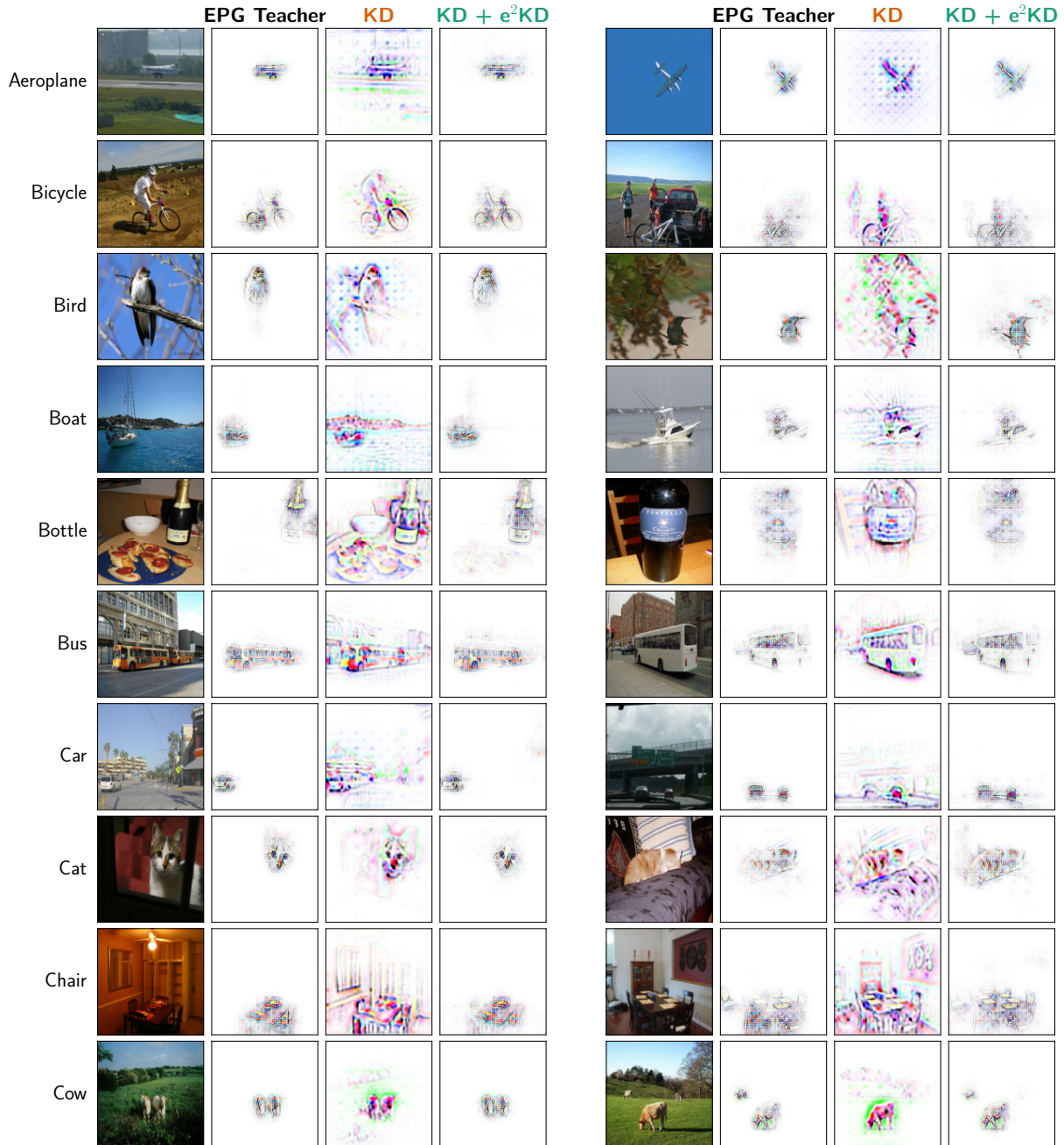


Figure A3. **Maintaining focused explanations (classes 1-10)**: Similar to Fig. 3 in the main paper, here we show qualitative difference of explanations. Each row shows two samples per class (for classes 11-20 see Fig. A4). We find that explanations of the student trained with  $e^2$ KD (subcol. 4 on both sides) is significantly closer to the teacher’s (subcol. 2), whereas vanilla KD students also focus on the background (subcol. 3). Samples were drawn from the test set with all models having correct predictions.

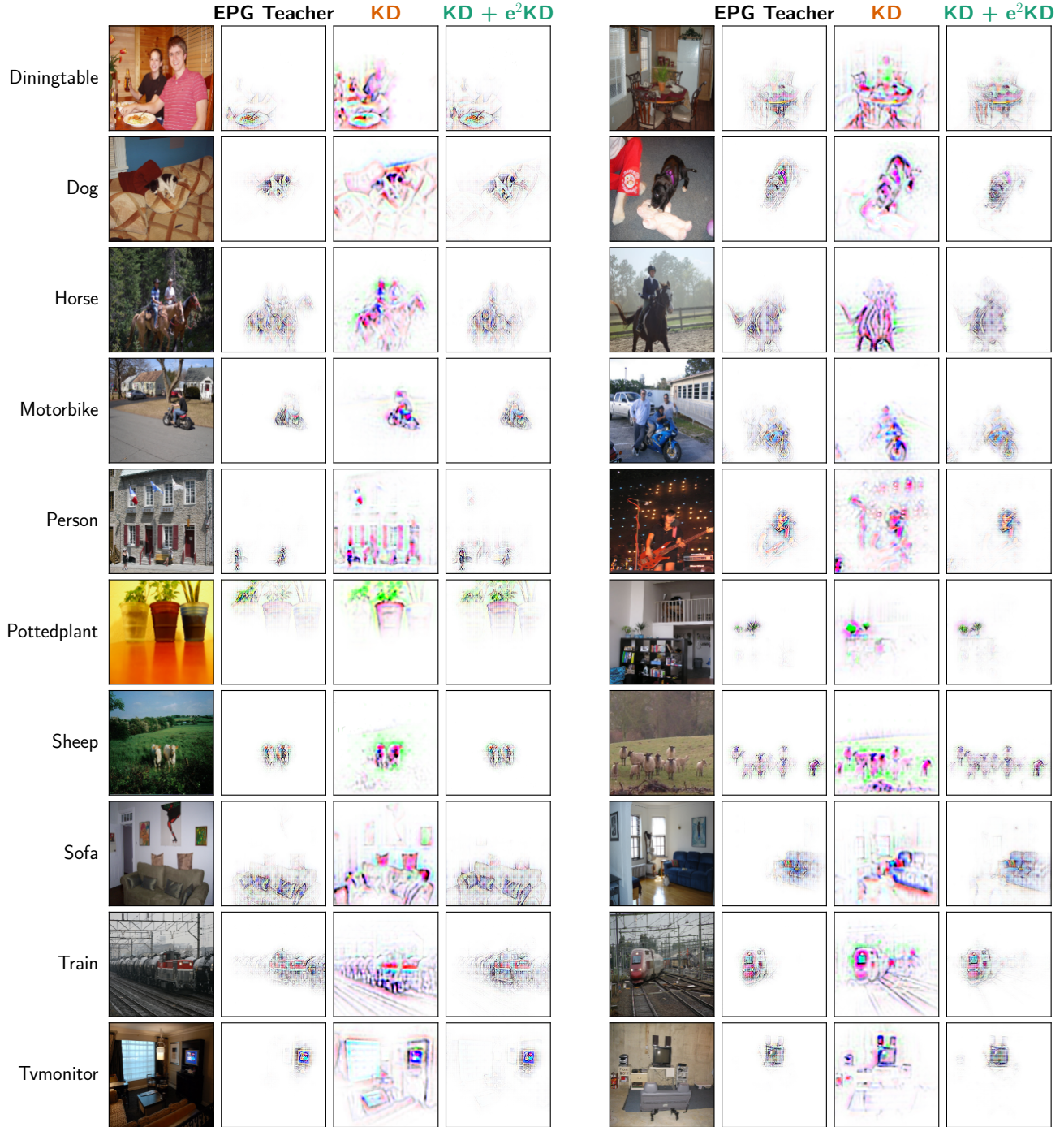


Figure A4. **Maintaining focused explanations (classes 11-20)**: Similar to Fig. 3 in the main paper, here we show qualitative difference of explanations. Each row shows two samples per class (for classes 1-10 see Fig. A3). We find that explanations of the student trained with e<sup>2</sup>KD (subcol. 4 on both sides) is significantly closer to the teacher's (subcol. 2), whereas vanilla KD students also focus on the background (subcol. 3). Samples were drawn from test set with all models having correct predictions.

### A.3. Distilling Architectural Priors

In this section, we provide additional qualitative samples for Sec. 4.3.2 in the main paper, where we distill a B-cos CNN to a B-cos ViT. Looking at Fig. A5, one can immediately observe the difference in interpretability of the B-cos ViT explanations when trained with  $e^2$ KD vs. vanilla KD. Additionally, following what was reported in Fig. 5, one can see that the ViT trained with  $e^2$ KD, similar to its CNN Teacher, maintains consistent explanations under shift, despite its inherent tokenization, whereas the explanations from vanilla KD significantly differ (compare every odd row to the one below).

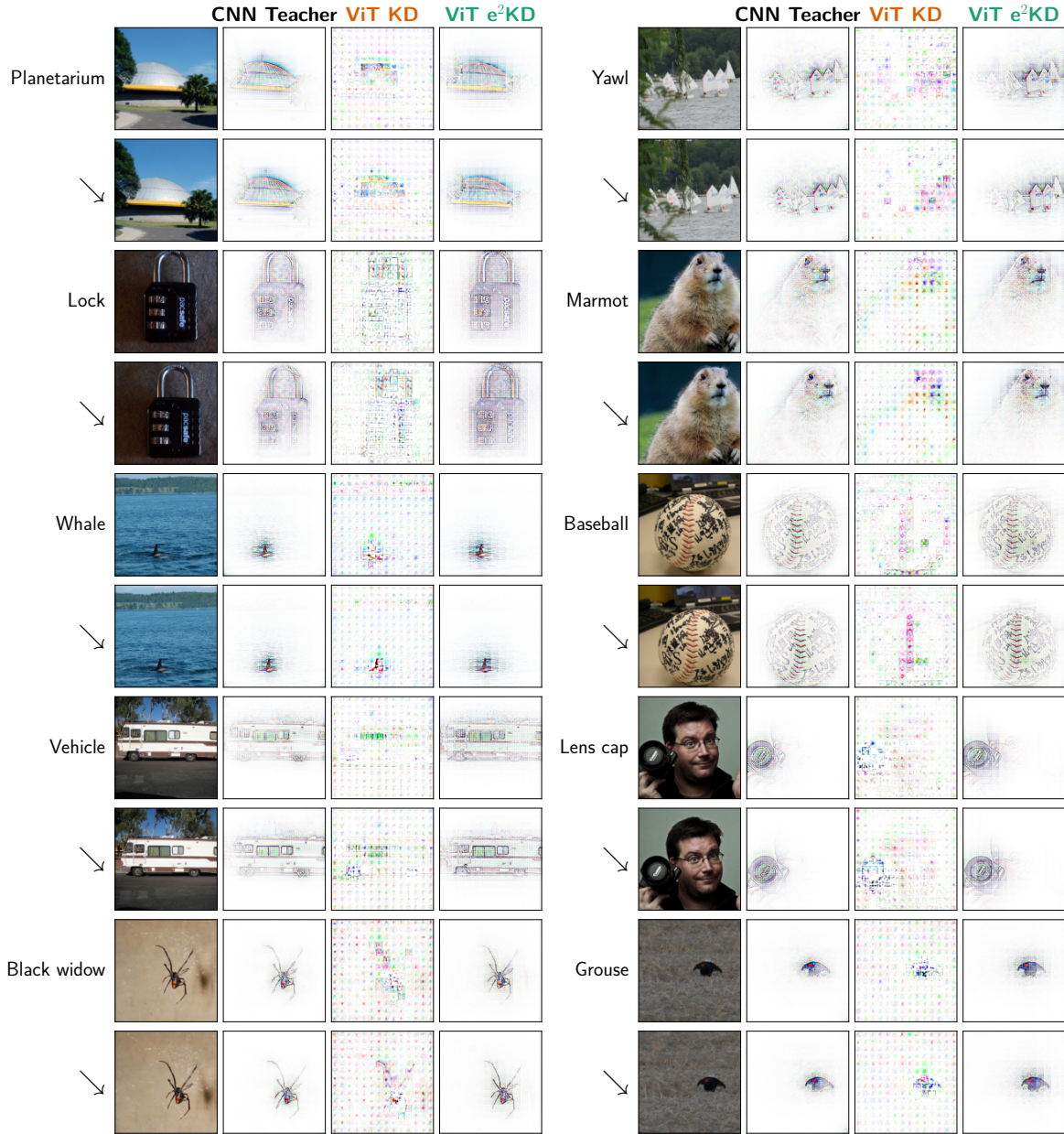


Figure A5. **Qualitative results on distilling B-cos DenseNet-169 to B-cos ViT<sub>Tiny</sub>.** We see that explanations of the  $e^2$ KD ViT student (col. 4 on both sides) is significantly more interpretable than vanilla KD student (col. 3 on both sides), and very close to the teacher’s explanations (col. 2 on both sides). We also shift every image diagonally to the bottom right by 8 pixels and show the explanations for the same class (rows indicated by ↙). We see that the explanations of the ViT student trained with  $e^2$ KD are equivariant under such a shift. In contrast, the ViT student from vanilla KD is sensitive to such shifts and the explanations change significantly.

## B. Additional Quantitative Results

### B.1. Reproducing previously reported results for prior work.

Since we use prior work on new settings, namely ImageNet with limited data, Waterbirds-100, and B-cos models, we reproduce the performance reported in the original works in the following. In particular, in Tab. B1, we report the results obtained by the training ‘recipes’ followed by prior work to validate our implementation and enable better comparability with previously reported results.

For this, we distilled the standard ResNet-34 teacher to a ResNet-18 on ImageNet for 100 epochs, with an initial learning rate of 0.1, decayed by 10% every 30 epochs. We used SGD with momentum of 0.9 and a weight-decay factor of  $1e-4$ . For AT and ReviewKD, we followed the respective original works and employed weighting coefficients of  $\lambda \in \{1000.0, 1.0\}$  respectively. For CAT-KD, we used  $\lambda \in \{1.0, 5.0, 10.0\}$  after identifying this as a reasonable range in preliminary experiments.

Following [21], we also report the results for KD in which the cross-entropy loss with respect to the ground truth labels is used in the loss function. We were able to reproduce the reported numbers by a close margin. Our numbers are also comparable to the torchdistill’s reproduced numbers [27], see Tab. B1. We see that  $e^2$ KD again improves both accuracy and agreement of vanilla KD (agreement 80.2 $\rightarrow$ 80.5). Also note that the vanilla KD baseline significantly improves once we used the longer training recipe from [4] in Tab. 1 in the main paper (accuracy 70.6 $\rightarrow$ 71.8; agreement 80.2 $\rightarrow$ 81.2).

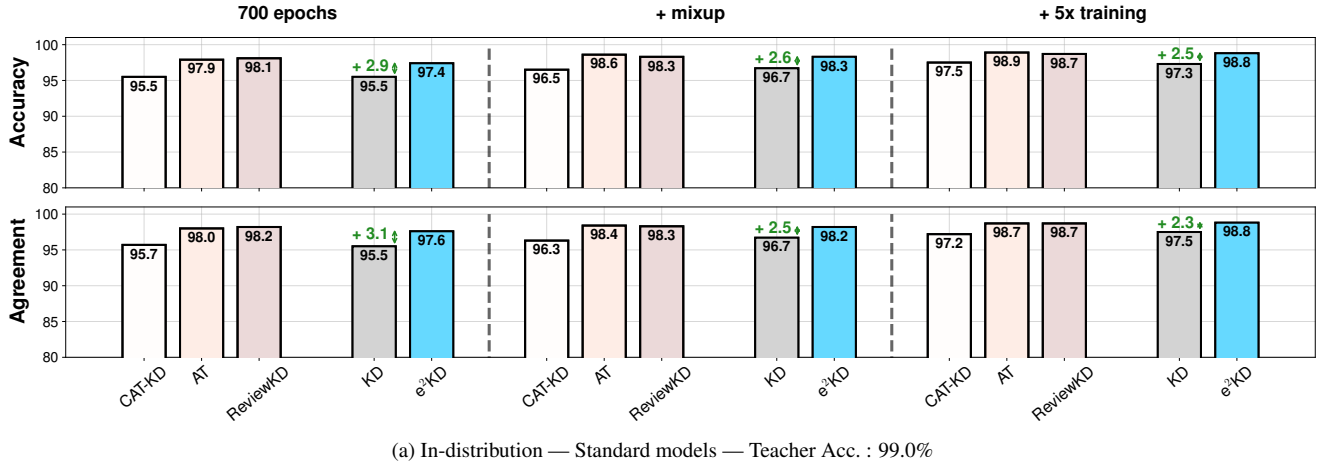
<b>Standard Models</b> Teacher ResNet-34 Accuracy 73.3%	Accuracy	Agreement	Reported Accuracy	torchdistill Accuracy
KD [21] (with cross-entropy)	71.0	79.7	70.7	71.4
AT [45]	70.2	78.3	70.7	70.9
ReviewKD [9]	71.6	80.1	71.6	71.6
CAT-KD [19]	71.0	80.1	71.3	-
KD	70.6	80.2	-	-
<b>+ <math>e^2</math>KD (GradCAM)</b>	<b>70.7 (+ 0.1)</b>	<b>80.5 (+ 0.3)</b>	-	-

Table B1. **Distilling Standard ResNet-34 to ResNet-18 for reproducing prior work.** We verify our implementation of prior work by distilling them in the 100 epoch setting used in [9, 19, 45]. We observe that our accuracy is very close to the reported one and the reproduced numbers by torchdistill [27]. We also see that  $e^2$ KD, similar to Tab. 1, improves accuracy and agreement of vanilla KD.

## B.2. Full results on Waterbirds — B-cos and conventional models on in- and out-of-distribution data

In this section we provide complete quantitative results on Waterbirds-100 dataset [30, 36], for both standard and B-cos models. In Fig. B1, we report in-distribution accuracy and agreement. We observe that all models are performing well on in-distribution data (lowest test-accuracy is 94.9% for standard and 95.5% for B-cos models.). Nevertheless, e<sup>2</sup>KD is again consistently providing gains over vanilla KD. More importantly however, for the out-of-distribution samples, as reported in Fig. B2, we observe that e<sup>2</sup>KD offers even larger accuracy and agreement gains over vanilla KD for both standard and B-cos models. Corresponding qualitative results, for the 700 epoch experiments, can be found in Fig. A1, for in-distribution, and Fig. A2 for out-of-distribution samples.

### In-distribution data — Standard Models



### In-distribution data — B-cos Models

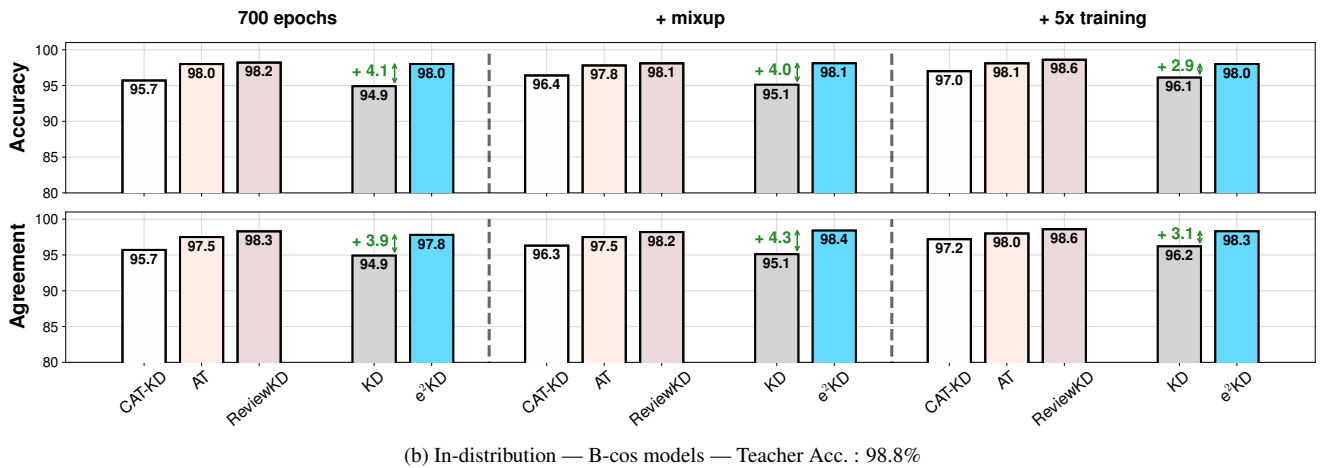


Figure B1. **KD on in-distribution data for standard (a) and B-cos (b) models on Waterbirds-100.** We show accuracy (top rows) and agreement (bottom rows) when distilling from ResNet-50 teachers to ResNet-18 students with various KD approaches. As for out-of-distribution data (see Fig. B2), we find significant and consistent gains in accuracy and agreement on in-distribution for both model types.

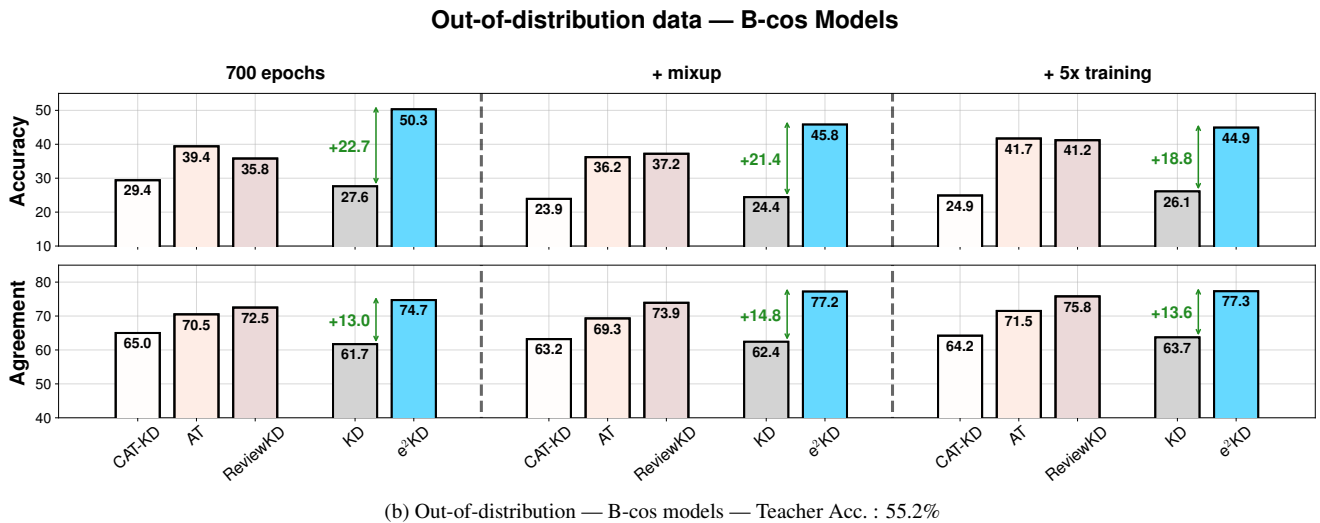
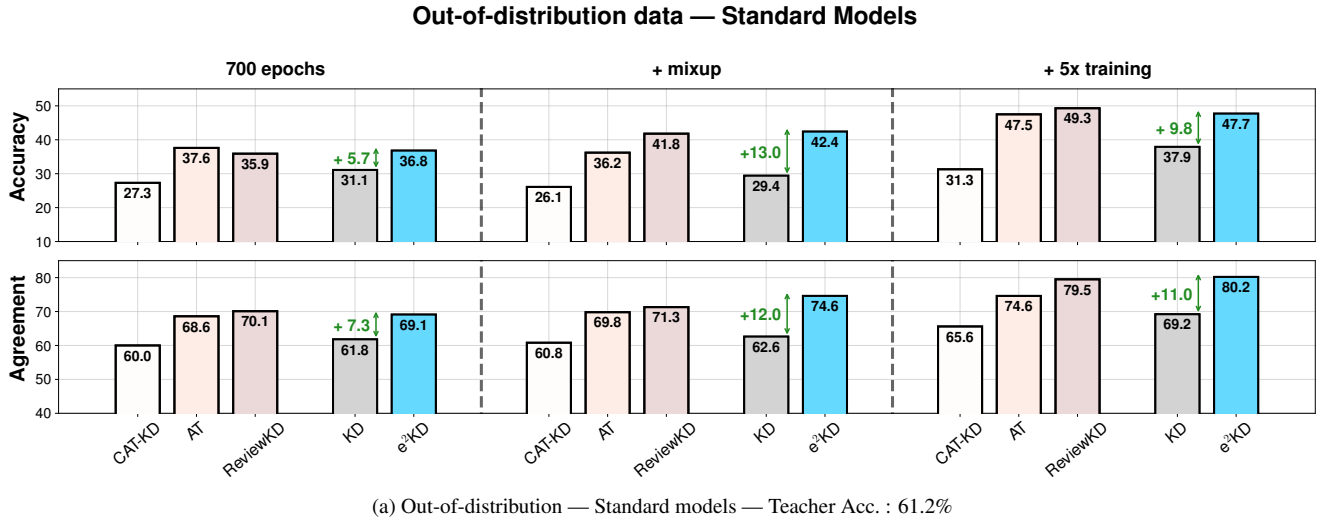


Figure B2. **KD on out-of-distribution data for standard (a) and B-cos (b) models on Waterbirds-100**; note that (a) is the same as Fig. 4 in the main paper and repeated here for easier reference. We show accuracy (top rows) and agreement (bottom rows) when distilling from ResNet-50 teachers to ResNet-18 students with various KD approaches. Similar as for the standard models (a), we find that e<sup>2</sup>KD also significantly increases both accuracy and agreement for B-cos models. For results on in-distribution data, please see Fig. B1.

## C. Implementation Details

In this section, we provide additional implementation details. In Sec. C.1, we provide a detailed description of our training setup, including hyperparameters used in each setting. In Sec. C.2, we describe how we adapt prior approaches that were proposed for conventional deep neural networks to B-cos models. Code for all the experiments will be made available<sup>4</sup>.

### C.1. Training Details

In this section, we first provide the general setup which, unless specified otherwise, is shared across all of our experiments. Afterwards, we describe dataset-specific details in Secs. C.1.1 to C.1.3, for each dataset and experiment.

**Standard Networks.** As mentioned in Sec. 4 in the main paper, we follow the recipe from [4]. For standard models, we use the AdamW optimizer [23] with a weight-decay factor of  $10^{-4}$  and a cosine-annealing learning-rate scheduler [24] with an initial learning-rate of 0.01, reached with an initial warmup for 5 epochs. We clip gradients by norm at 1.0.

**B-cos Networks.** We use the latest implementations for B-cos models [6]. Following [5, 6], we use the Adam optimizer [23] and do not apply weight-decay. We use a cosine-annealing learning-rate scheduler [24] with an initial learning-rate of  $10^{-3}$ , reached with an initial warmup for 5 epochs. Following [6], we clip gradients using adaptive gradient clipping (AGC) [7].

Unless specified otherwise, across all models and datasets we use random crops and random horizontal flips as data augmentation during training, and at test time we resize the images to 256 (along the smaller dimension) and apply center crop of (224, 224). We use PyTorch [29] and PyTorch Lightning [16] for all of our implementations.

#### C.1.1 ImageNet Experiments

For experiments on the full ImageNet dataset [12], we use a batch size of 256 and train for 200 epochs. For limited-data experiments we keep the number of steps same across both settings (roughly 40% total steps compared to full-data): when using 50 shots per class, we set the batch size to 32 and train for 250 epochs, and when having 200 shots, we use a batch size of 64 and train for 125 epochs. We use the same randomly selected shots for all limited-data experiments. For data-free experiments (Tab. 5 in the main paper), following [4], we used equal number of training steps for both SUN→IMN (125 epochs with a batch size of 128) and IMN→SUN (21 epochs with a batch size of 256).

For the pre-trained teachers, we use the Torchvision checkpoints<sup>5</sup> [26] for standard models and available checkpoints for B-cos models<sup>6</sup> [6]. For all ImageNet experiments, we pick the best checkpoint and loss coefficients based on a held-out subset of the standard train set, which has 50 random samples per class. The results are then reported on the entire official validation set. We use the following parameters for each method:

Standard Networks (Tab. 1)		B-cos ResNet-34 Teacher (Tab. 2)	
KD	$\tau \in [1, 5]$	KD	$\tau \in [1, 5]$
e <sup>2</sup> KD	$\tau \in [1, 5], \lambda \in [1, 5, 10]$	e <sup>2</sup> KD	$\tau \in [1, 5], \lambda \in [1, 5]$
AT	$\lambda \in [10, 100, 1000, 10000]$	AT	$\lambda \in [1, 10, 100, 1000]$
ReviewKD	$\lambda \in [1, 5]$	ReviewKD	$\lambda \in [1, 5]$
CAT-KD	$\lambda \in [1, 5, 10]$	CAT-KD	$\lambda \in [1, 5, 10]$

B-cos DenseNet-169 Teacher (Tab. 3)		B-cos DenseNet-169 to ViT Student (Fig. 5)	
KD	$\tau \in [1, 5]$	KD	$\tau \in [1, 5]$
e <sup>2</sup> KD	$\tau \in [1, 5], \lambda \in [1, 5, 10]$	e <sup>2</sup> KD	$\tau \in [1], \lambda \in [1, 5, 10]$
* KD	$\tau \in [1, 5]$		
* e <sup>2</sup> KD	$\tau \in [1, 5], \lambda \in [0.2, 1, 5, 10]$		
Data-free (Tab. 5) KD	$\tau \in [1, 5]$		
Data-free (Tab. 5) e <sup>2</sup> KD	$\tau \in [1, 5], \lambda \in [1, 5, 10]$		

For ViT students we trained for 150 epochs, and following [6], we used 10k warmup steps, and additionally used RandAugment[11] with magnitude of 10.

<sup>4</sup><https://github.com/m-parchami/GoodTeachersExplain>

<sup>5</sup><https://pytorch.org/vision/stable/models.html>

<sup>6</sup><https://github.com/B-cos/B-cos-v2>

### C.1.2 Waterbirds Experiments

For the Waterbirds [36] experiments, we use the 100% correlated data generated by [30] (i.e. Waterbirds-100). We use the provided train, validation and test splits. Since the data is imbalanced (number of samples per class significantly differ), within each sweep we pick the last-epoch checkpoint with best *overall* validation accuracy (including both in-distribution and out-of-distribution samples). We use batch size of 64. For experiments with MixUp, we use  $\alpha=1$ . The pre-trained guided teachers were obtained from [32]. For applying AT and ReviewKD between the ResNet-50 teacher and ResNet-18 student, we used the same configuration from a ResNet-34 teacher, since they have the same number of blocks.

We tested the following parameters for each method:

Standard models (Fig. 4 and Sec. B.2)		B-cos models (Fig. 2 and Sec. B.2)	
KD	$\tau \in [1, 5]$	KD	$\tau \in [1, 5]$
e <sup>2</sup> KD	$\tau \in [1, 5], \lambda \in [1, 5, 10, 15]$	e <sup>2</sup> KD	$\tau \in [1], \lambda \in [1, 5, 10]$
AT	$\lambda \in [10, 100, 1000]$	AT	$\lambda \in [10, 100, 1000]$
ReviewKD	$\lambda \in [1, 5, 10, 15]$	ReviewKD	$\lambda \in [1, 5, 10]$
CAT-KD	$\lambda \in [1, 5, 10, 15]$	CAT-KD	$\lambda \in [1, 5, 10]$

### C.1.3 PASCAL VOC Experiments

We use the 2012 release of PASCAL VOC dataset [14]. We randomly select 10% of the train samples as validation set and report results on the official test set. We use batch size of 64 and train for 150 epochs. The pre-trained guided teachers were obtained from [32]. Since we are using VOC as a *multi-label* classification setting, we replace the logit loss from Eq. (1) in the main paper with the logit loss recently introduced by [43]:

$$\mathcal{L}_{MLD} = \tau \sum_{j=1}^c D_{\text{KL}} \left( \left[ \psi_j \left( \frac{z_T}{\tau} \right), 1 - \psi_j \left( \frac{z_T}{\tau} \right) \right] \parallel \left[ \psi_j \left( \frac{z_S}{\tau} \right), 1 - \psi_j \left( \frac{z_S}{\tau} \right) \right] \right). \quad (\text{C.1})$$

Here,  $\psi$  is the sigmoid function and  $[\cdot, \cdot]$  concatenates values into a vector. Note that the original loss from [43] does not have a temperature parameter  $\tau$  (i.e.  $\tau = 1$ ). For consistency with other experiments, here we also included a temperature factor. When reporting the final results on the test set, we resize images to (224, 224) and do not apply center crop. For the EPG and IoU metrics, we use the implementation from [32]. For the IoU metric, we use threshold of 0.05. We tested the following parameters for each method:

B-cos models (Tab. 4)	
KD	$\tau \in [1, 5]$ ,
e <sup>2</sup> KD	$\tau \in [1, 5], \lambda \in [1, 5, 10]$

## C.2. Adapting Prior Feature-based Methods for B-cos Models

While prior feature-based KD methods have been mainly introduced for conventional networks, in Tab. 2 we additionally tested them on B-cos networks. We applied them with the same configuration that they were originally introduced as for ResNet-34 [20] teacher and ResNet-18 student, with minor adjustments. Specifically, since B-cos networks also operate on negative subspace, we did not apply ReLU on the intermediate tensors in AT. For ReviewKD, since the additional convolution and norm layers between the teacher and student are only needed to convert intermediate representations, we used standard convolution and BatchNorm and not B-cos specific layers. For AT, ReviewKD, and CAT-KD we replaced the cross-entropy loss, with the modified binary cross entropy from [6].